Tuijin Jishu/Journal of Propulsion Technology
ISSN: 1001-4055
Vol. 45 No. 3 (2024)

Optimizing the Factors of Abrasive Water Jet Machining for Reinforced Al7075 Material Matrix Composite

C.Sravanthi[1*], S.Gajanana[2], A. Krishnaiah[3], Ch.Venkateswarlu[4]

[1]*Department of Mechanical Engineering, Anurag University, Hyderabad, India*

[2]*Department of Mechanical Engineering, M.V.S.R. Engineering College, Hyderabad, India*

[3]*Department of Mechanical Engineering, OUCE, Osmania University, Hyderabad, India*

[4]*Department of Research, Scientist 'F', DRDL, Kanchanbagh, Hyderabad, India*

Abstract:

This study investigates the enhancement of productivity in the aerospace industry through the optimized machining of Al7075-based Metal Matrix Composites (MMCs) reinforced with TiO2, ZnO, B4C, MgO, and B4N. Utilizing a Taguchi-based Multi-objective Response Surface Methodology (MORSM), the research identifies optimized parameters for Abrasive Water Jet Machining (AWJM) of these MMCs. A systematic experiment design using the Taguchi method allows for the variation of parameters, while contour-plot analysis facilitates data examination. The MORSM approach identifies machining parameters that significantly improve the Material Removal Rate (MRR). Validation experiments confirm the practical applicability and accuracy of the optimized parameters by comparing experimental and simulated results. This study highlights efficient machining parameters for various reinforcements in Al7075-based MMCs, demonstrating the method's reliability and utility in advancing aerospace material machining, thereby contributing to superior productivity and performance in aerospace application.

Keywords: Abrasive Water Jet Machining, Material Matrix Composites, Taguchi method, Signal to Noise ratio analysis, Contour-plot analysis, Trade-off analysis

1. Introduction

In the realm of advanced manufacturing, Abrasive Water Jet Machining (AWJM) has emerged as a cutting-edge technology that offers precision, versatility, and environmental sustainability. The importance of AWJM in contemporary industry cannot be overstated, as it addresses an array of production challenges and aligns with the growing emphasis on sustainable and efficient manufacturing processes.

At the core of AWJM lies a deceptively simple but remarkably effective process. Water is pressurized to extreme levels, typically between 60,000 and 90,000 PSI, and combined with abrasive particles, often garnet. The resulting abrasive water jet possesses an exceptional capacity for material removal through erosion. This results in precise cuts with minimal heat-affected zones, enabling intricate and detailed designs [1]. The process is characterized by its accuracy and adaptability, making it an ideal choice for applications where precision is paramount.

In the automotive industry, AWJM is invaluable for cutting and shaping metal parts, reducing material wastage, and enhancing efficiency. Furthermore, the medical field benefits from this technology, as it enables the creation of finely detailed surgical instruments, improving patient outcomes. Notably, AWJM can cut through a broad spectrum of materials, including delicate substances such as glass and composites, positioning it as an essential tool in numerous manufacturing processes [2].

1.1. Novelty and motivations

From the literature reviewed for the present study, it is observed that the MRR is the most crucial factor for productivity. MMC prepared with Al7075 as base material with reinforcements is mostly used Aerospace industries. However in Aerospace industries different MMCs are prepared by varying the reinforcements. This motivated the study to determine a set of process parameters of AWJM for machining Al7075 based MMC reinforced with TiO_2, ZnO, B_4C, MgO and B_4N prepared by the stir casting process. The objective of the present study is to determine a common set of machining parameters which compute the optimal or near optimal MRR values for all the five different MMC prepared. In order to achieve the objective of the paper, the problem is laidin a Multi-objective Optimization settings. Therefore, a Taguchi based Multi-objective Response Surface Methodology (MORSM) model is developed for achieving the objective of the paper. The present study also performs a parametric investigation of the result obtained from the experimentation to validate and confirms the

ptimized values. The flowchart for the study is shown in figure

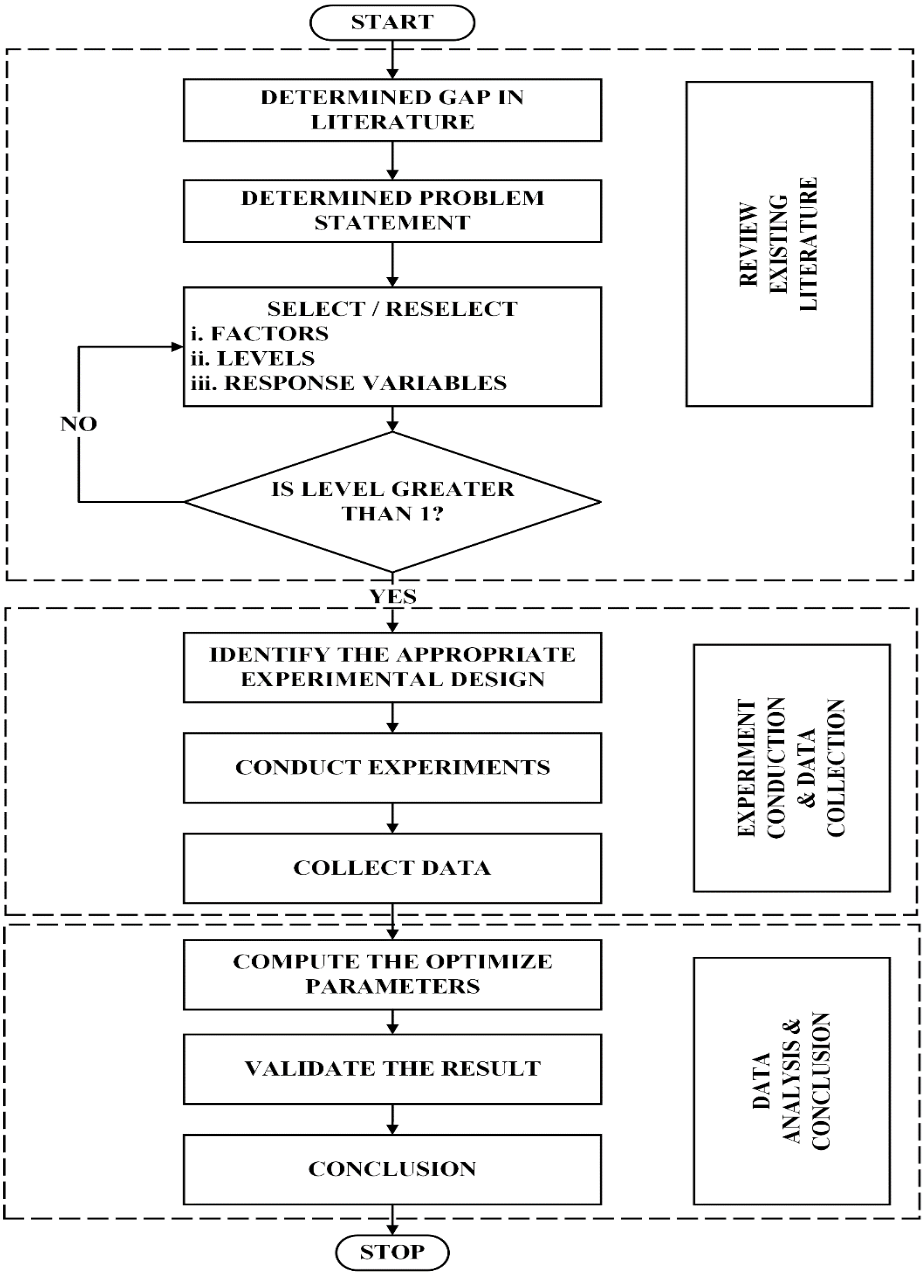

1.

Figure 1: Flowchart of the study

2. Literature Review

The literature on the optimization of factors for machining AWJM is extensive and comprehensive. Researchers have conducted numerous studies to evaluate the key parameters that influence the performance and efficiency of AWJM processes. These investigations have resulted in a significant quantity of published literature, providing a wealth of information for practitioners and academics alike.

The initial exploration of the available literature reveals a wide range of research articles, conference papers, and thesis publications that delve into different aspects of optimizing factors for AWJM. These publications address diverse topics such as nozzle geometry [19], abrasive type and concentration [20], standoff distance [21], pressure [22] and feed rate settings [23], and material characteristics [24]. Such a broad array of literature demonstrates the comprehensive nature of research in this field, indicating a depth of knowledge and an active interest from the academic community.

In summary, the literature on the optimization of factors for machining Abrasive Water Jet Machining is abundant, diverse, and continually growing. The numerous publications indicate a comprehensive understanding of the field and the active involvement of the academic community. In this study, the literature reviewed is mostly done on in 4 parts viz. a) papers on the **o**ptimization techniques for AWJM parameters, b)effect of abrasive properties on machining performance, c) workpiece material considerations and surface integrity, d) nozzle design and its impact on machining quality and e) environmental sustainability and AWJM.

In [25], the paper determines the optimal combination of AWJM parameters with the use of Taguchi method with the objective of improving machining performance. The authors conducted experiments and analyzed the effects of various parameters such as abrasive flow rate (AFR), standoff distance (SoD), and traverse speed (TS) on the machining characteristics. The results showed that the Taguchi method effectively optimized the parameters and enhanced the machining performance. In [26], paper investigates the optimization of AWJM parameters using response surface methodology (RSM). The authors conducted experiments to determine the effects of parameters such as AFR, SoD, and TS on the machining characteristics. The RSM was employed to develop mathematical models and optimize the parameters. The findings demonstrated that RSM effectively optimized the parameters and improved the machining performance. In paper [27], focuses on the multi-objective optimization of AWJM parameters using multi-objective Jaya (MO-Jaya)algorithm and PROMETHEE method. The authors conducted experiments to determine the effects of parameters such as AFR, SoD, and TS on multiple performance characteristics. The algorithms were employed to optimize the parameters and find the best compromise solution. The results showed that the methods effectively optimized the parameters and achieved improved performance in terms of MRR, surface roughness (SR) and kerf taper. In paper [28], investigates the optimization of AWJM parameters for α-β brass using a Taguchi algorithm. The authors conducted experiments to determine the effects of parameters such as AFR, SoD, and TS on the machining characteristics. The Taguchi optimization was employed to optimize the parameters and find the optimal combination. The findings demonstrated that the Taguchi optimization effectively optimized the parameters and improved the machining performance.

In paper [29], presents the optimization of AWJM parameters using multi-objective particle swarm optimization (MOPSO). The authors conducted experiments to study the effects of AFR, SoD, and TS on the machining performance. The MOPSO algorithm was employed to determine the optimal parameter combination considering multiple objectives. The study concludes that the AFR and SoD significantly influence the machining performance, while the TS has a relatively smaller effect. In paper [30], the authors investigates the effects of parameters such as AFR, SoD, and TS on the machining performance in AWJM using Taguchi method. L9 orthogonal array was generated and analyzed the results using signal-to-noise ratio (S/N) and analysis of variance (ANOVA). The study concludes that the optimal combination of process parameters significantly affects the machining performance and surface quality in AWJM. In paper [31], focused on the optimization of AWJM process parameters using RSM. The study aims to determine the optimal combination of process parameters, including AFR, SoD, and TS, to achieve improved machining performance. The authors conducted experiments based on a central composite design and developed response surface models to predict the machining performance characteristics. The results indicate that RSM is an effective approach for optimizing process parameters in AWJM.In [34], examined the MRR effect in the process of abrasive water jet machining while varying the input parameters, including nozzle tilted angle, water pressure, jet feed speed, and abrasive mass flow rate. They discovered that when water pressure and mass flow rate rise due to alumina ceramic cutting, the MRR increases.

In AWJM, material removal rate (MRR) is one of the most important performance measures. MRR is the measure of material removed from the parent workpiece per unit time. MRR is important because it defines the productivity of the machining process [32]. The MRR is crucial for surface integrity, cutting forces and temperatures, spindle power, deflections, and the workpiece's dimensional and form accuracy. The AWJM is mostly used to attain the dimensional accuracy while machining [33]. In paper [35], the optimized processing parameters are computed for minimizing the average SR and delamination damage values for drilling glass fiber-reinforced polymer composite material (GFPCM) by AWJM process. Many other papers were reviewed for the study but limiting to the most recent and important papers.

3. Experimental setup and material

In this section of the study discusses about the experimental setup and the material used for the study.

3.1. Experimental setup

Abrasive Water Jet Machining (AWJM) is a cutting-edge technology employing water pressures exceeding 40,000 psi or 2760 bar to achieve precise material removal. In this waterjet cutting system, pressurized water is channeled through a cutting nozzle containing an orifice assembly housing a small-hole jewel, typically crafted from high-strength materials like sapphire or diamond. As the water passes through this jewel, it accelerates to remarkable speeds of up to 2,500 feet per second, entering a larger chamber where it creates a suction force, drawing abrasive material into the stream. The abrasive is stored in a hopper positioned on the X-Y table, with an air-operated sanding valve releasing it into a feed tube that directs it into the nozzle. Within the abrasive jet nozzle, the high-pressure water, regulated by an ON/OFF valve, is forced through a small hole in the jewel, initiating the mixing process with abrasive particles in a hard and brittle mixing tube designed to withstand abrasion. At the bottom of this tube, water and abrasive combine to form a rapid suspension, creating a slurry that functions akin to a cutting tool when propelled onto the material surface by the high-speed jet. The AWJM system utilized in this study adheres to stringent pressure and flow rate specifications, ranging from 75 to 120 psi (517 to 827 kPa) and maintaining a minimum flow rate of 16.0 cfm (453 l/m). Figure 2 provides a labeled diagram depicting the components and arrangement of this innovative AWJM system employed for experimental purposes.

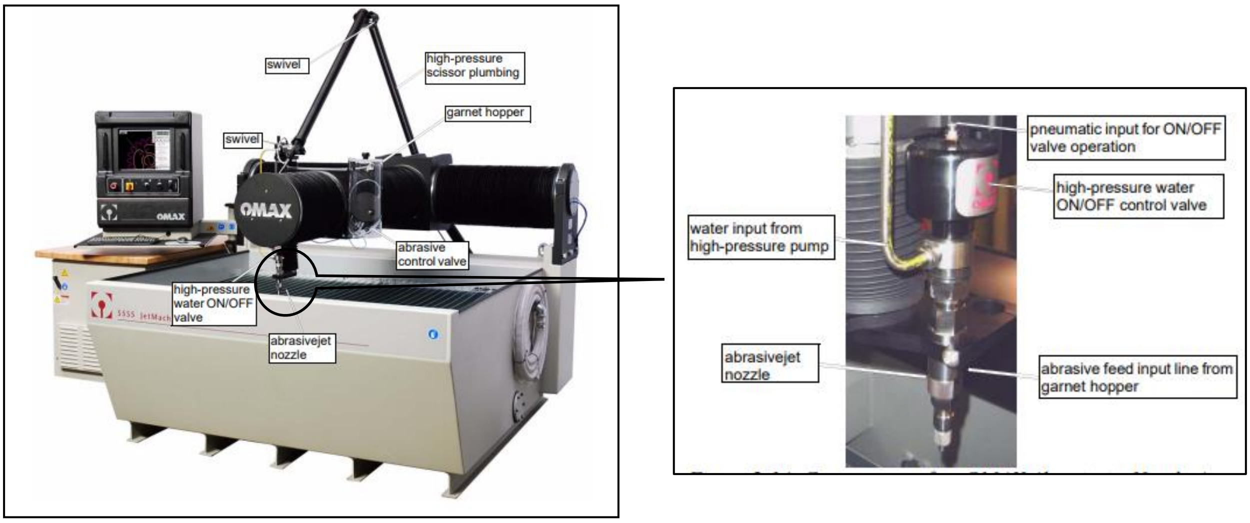

Figure 2:Abrasive Water Jet Machine with the abrasive jet nozzle

3.2. Material used for the experimentation

In this study, Aluminium alloy 7075 (Al7075) based Material Matrix Composite (MMC) is prepared with Boron Carbide (B_4C), Zinc Oxide (ZnO), Titanium dioxide (TiO_2), Magnesium Oxide (MgO) and Boron Nitride (B_4N) as reinforcement. The MMC is prepared in an induction furnace by the ex-situ stir casting process. The reinforcements having 99.9% purity with 325 mesh size and commercially available Al7075 were used as raw materials which are melted in a graphite crucible in an induction furnace. 5 different specimens are prepared for each reinforcement separately and each having dimension of $30 \times 30 \times 100$ mm. The Al7075 is chosen as the base material because of its physical and chemical properties. The physical properties of the Al7075 depends greatly on the tempering of the material. The Al7075 used in the study is tempered by T6 method. The physical properties and chemical composition of Al7075-T6 is shown in table 1 and2 respectively.

Table 1: Table showing the physical properties of Al7075 – T6

Property	Density $\left({gm}/{cm^3}\right)$	Young's Modulus (GPa)	Tensile strength (MPa)	Elongation at break (%)	Poisson's ratio	RockwellH ardness (HRB)	Melting temperature (℃)
Values	2.81	71.7	572	11	0.33	87	477

Table 2: Table showing the chemical composition of Al7075

Element	**Cu**	**Cr**	**Mn**	**Mg**	**Si**	**Ti**	**Zn**	**Fe**	**Al**
Percentage (%)	1.8	0.2	0.4	1.9	0.5	0.15	3.25	0.5	91.3

The commercial grade Al7075 is first melted at a temperature of 685℃ and preheated reinforcement is added in a control manner to the molten metal manually with the help of spatula. For obtaining homogenized mixture is constantly stirred at 200–300rpm for approximately 10 min by a mechanical stirrer. In order to remove the dissolved gases from the molten mixture a small quantityofC_2Cl_6 is added just 2 – 3 minutesbefore pouring the molten metal to a cuboidal mould of size $40 \times 40 \times 100$ mm. Figure 3 shows the isometric view of the specimen prepared for the study. From the prepared specimen experimental material of size $15 \times 15 \times 40$ mm is cut. A tolerance of 5 mm and 10 mm is kept in both horizontal and vertical axes of the specimen.The same process is repeated by differing the reinforcements

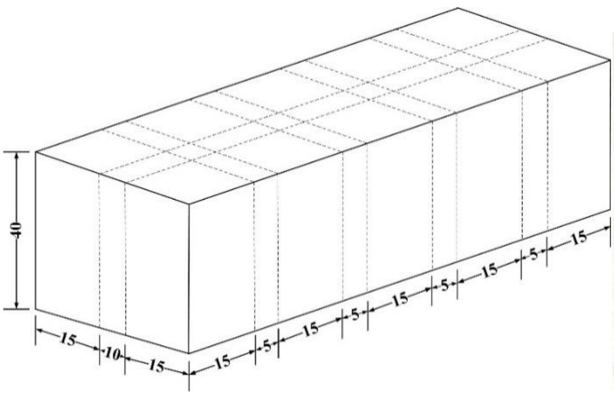

(a)

(b)

Figure 3: The figure shows the (a) isometric drawingand (b) isometric view of the experimental material prepared from the mould.

3. 3. Parametric study of the AWJM process

The abrasive water jet machining process is simulated by the Fluent workbench of Ansys. In this regard, the base material is set as Al-7075. Figure 4 shows the simulation of the flow rate of the AWJM for maximum

---

MRR. From figure 4, it is observed that the material is at maximum stress when the zone where the water jet hits the material. The velocity around that zone varies about 6135 – 6902 ms^{-1}

The turbulence kinetic energy (TKE) is simulated by Ansys Fluent is shown in figure 5. The zone where the water jet hits the material have the highest value of TKE. It confirms the fact that the maximum amount of material is removed from the base material is due to the TKE. After hitting the water swirls around the material in symmetric order thereby losing the TKE and due to which no material is removed from the other parts of the base metal.

The volume fraction of water is simulated by the ANSYS software. The volume fraction of water is the amount of water present in the mixture of water, abrasive particles and air at the nozzle exit. The simulation is shown in figure 6. From the figure 6, it is observed that for maximum amount of material to be removed from the base metal, the volume fraction of water to be set must be in the range of 24.49% to 30.61%.

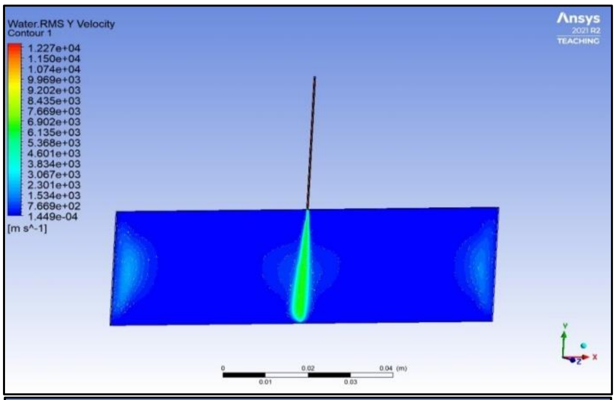

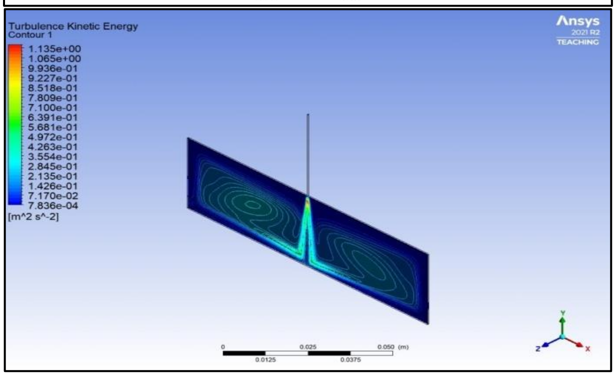

Figure 4: Flow rate simulation of the AWJMFigure 5: TKE simulation of the AWJM

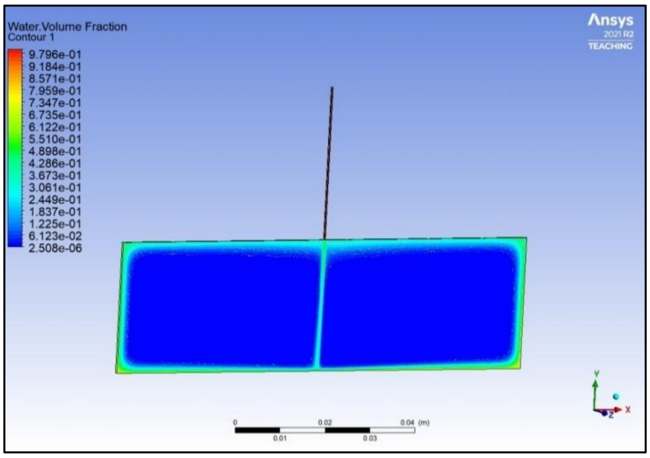

Figure 6: Water volume fraction simulation of the AWJM

3.4. Design of experiment (DOE)

DOE is defined as the study application of statisticsthat deals with the processes of designing, conducting and gathering of information and drawing a causal nexus between the performance and process parameters. In DOE, the controllable factors or the process parameters are varied and the output value is monitored throughout the procedure thereby determining the relationship between the factors and outputs [3]. There are several methods for creating DOE. Out of all the, Taguchi method outstand because it designs the least number of experiments [4].

The Taguchi DOE method plans the sturdiest experimental design. The Taguchi methodology aims in computing the optimal parameter settings so the process is not affected by noise [5]. The Taguchi DOE method creates an orthogonal array of experiment based on the process parameters and levels.

Based on the parametric study, the flow rate of the water jet is set at 3200 ms^{-1} and water volume fraction is 25%. Whereas, in this study, pressure of the water jet (PWJ) in bar, SoD in mm, and TS in mm/min are varied and these are the different process parameters which are designed for three levels as shown in table 3. The orthogonal array created for the experiment and the values of the output is shown in table 4.

Table 3: Levels for the experiments

Process parameters	**PWJ** $(\boldsymbol{bar})$	**SoD** $(\boldsymbol{mm})$	**TS** $(\boldsymbol{mm}/\boldsymbol{min})$
Level 1	1800	1	46.45
Level 2	2800	1.5	68.92
Level 3	3800	2	80.21

3.5. Performance parameter and its measurement

In industries, productivity is a crucial factor. Maximizing MRR means higher productivity and faster turnaround times. This is especially important when producing components or products from aluminum alloys and composite materials, as it can lead to cost savings and reduced lead times.When studying materials like Al7075 with reinforcements, researchers and engineers often aim to optimize the machining process for better performance. MRR is a key parameter to be optimized, as it reflects the effectiveness of the cutting tool, cutting parameters, and the overall machining strategy.

High MRR can generate more heat during machining, which can affect the material properties, especially in the case of composite materials. Understanding the thermal effects and their impact on the work-piece and tool is crucial for process control.MRR is often used to guide the selection of cutting tools and the determination of appropriate cutting parameters (e.g., cutting speed, feed rate, depth of cut). Researchers may want to find the optimal combination of these factors to achieve the desired MRR without compromising tool life or work-piece quality.

In summary, MRR is a critical output response in the study of materials like Al7075 with reinforcements because it directly relates to the efficiency, productivity, and overall effectiveness of machining processes. Optimizing MRR can lead to improved manufacturing processes and reduced costs while considering factors like tool life, surface finish, and thermal effects.The output for the experiment in this study is the MRR which is calculated as per Eq. (1).

$$MRR = \frac{m_i - m_f}{t} \qquad (1)$$

Where m_i and m_f are mass before the start and after completion of machining respectively and t is the time taken for completion of the machining process.

Table 4: Performance values for the conducted experiments.

Exp. no.	**PWJ** (bar)	**SoD** (mm)	**TS** (mm/min)	**MRR** (gm/min)				
				Al7075+TiO_2	**Al7075+ZnO**	**Al7075+B_4C**	**Al7075+MgO**	**Al7075+B_4N**
1	1800	1	46.45	5.555	3.703	1.851	1.851	3.703
2	1800	1.5	68.92	5.964	5.964	3.976	3.976	5.964
3	1800	2	80.21	7.462	7.462	5.597	5.597	7.462
4	2800	1	68.92	12.5	12.5	12.5	10	12.5
5	2800	1.5	80.21	14.218	14.218	14.218	14.218	16.587
6	2800	2	46.45	17.5	20	17.5	17.5	20
7	3800	1	80.21	25	25	25	25	25
8	3800	1.5	46.45	27.692	30.769	24.615	27.692	30.769
9	3800	2	68.92	28.571	28.571	28.571	25.714	28.571

4. Methodology

In this section of the paper, the preliminary of the methodologies adopted for the analysis is explained in brief.

4.1. Analysis of Variance (ANOVA)

ANOVA is a statistical method used to compare means among multiple groups. It assesses whether group means are significantly different. In one-way ANOVA, a single factor's impact is examined on a continuous dependent variable. It calculates the F-statistic by comparing variation between groups to within-group variation. The null hypothesis is accepted or rejected based on the p – value as computed from the significance level (typically 0.05). If null hypothesis is rejected, it implies that at least one group mean differs significantly from the others [17]. In this study, ANOVA is used to determine the factors that have a significant effect on measured outcome i.e. the MRR.

4.2. Analysis of signal to noise ratio (S/N)

S/N analysis is based on robustness [6]. The objective of the analysis is to reduce the impact of noise by altering the controllable factors which are termed as sound [7]. The S/N is determined by the Taguchi loss-function which measures the deviation between the directly measured test values and the optimal machining values [8].The S/N values are computed based on the fact that the higher, lower or nominal values of the performance is desired [9]. The S/N values are computed as per the Eqs. (2 – 4).

i. Higher the better type: $S/_N = -10 * log\left[\frac{1}{n}\sum_{i=1}^{n}\left(\frac{1}{y_i}\right)^2\right]$ (2)

ii. Lower the better type: $S/_N = -10 * log\left[\frac{1}{n}\sum_{i=1}^{n}(y_i)^2\right]$ (3)

iii. Nominal the best: $S/_N = -10 * log(\sigma)^2$ (4)

Where y_i denotes the value of measured i^{th} response and σ denotes the value of standard deviation.

4.3. Contour plot analysis

Contour plot analysis is a method of representing 3-d graphical representation in 2-d view by plotting constant z slices, called contours, on a 2-dimensional format [10]. The contour plot analysis is used to show impact of the variation of two independent variables on the dependent variable [11]. The contour plots are color coded representing different intervals of the output with different colors.

4.4. Trade off analysis

Trade-off analysis is a decision-making process that involves evaluating the benefits and drawbacks of different options to make informed choices. It is especially useful when facing limited resources, as it helps prioritize one factor over another.In trade-off analysis, various criteria, such as cost, time, quality, or performance, are considered, and the trade-offs between them are assessed.Trade-off analysis is applied in areas from economics to pollution research [12 – 14]. MORSM is one of the most used trade-off model.

MORSM is a statistical and optimization technique used to simultaneously optimize multiple conflicting objectives in a complex system. It extends traditional RSM, which focuses on optimizing a single response variable [15]. In MORSM, multiple response variables are considered, and mathematical models are developed to represent the relationships between input factors and these responses. The goal is to find a set of input conditions that provide a trade-off solution, where improvements in one response may result in compromises in others. MORSM is particularly valuable in fields like engineering, manufacturing, and decision-making processes where several competing objectives need to be considered for optimal decision-making.MORSM value evaluates the best parameters by computing composite desirability value often denoted by (D). It varies in between 0 to 1 and value nearer to 1 is preferred [16]. In this study, a trade-off analysis is conducted to compute the optimal machining parameters that would return the best performance for all the prepared composites.

5. Result and discussions

In this section of the results obtained is discussed in details.

5.1. Result from ANOVA analysis

The first step of the analysis is statistically scrutinizing the significance of the input factors on MRR for each of the specimen prepared as described in the section 2.2. ANOVA analysis is used for hypothesis testing between the main effects and the performance. The significance of the factors are decided by the F-value which depends on their degree of freedom which is 2 for the present study. The F-value for (2, 8) with an upper confidence limit of 95% is 19.37. The ANOVA table for MRR for the five specimen prepared with reinforcement as TiO_2, ZnO, B_4C, MgO and B_4N are shown in table 5 – 9 respectively.

Table 5: ANOVA table for specimen with TiO_2 as reinforcement

Source	DF	Adj SS	Adj MS	F-Value	P-Value
PWJ	2	654.254	327.127	5135.43	0.000
SoD	2	18.337	9.169	143.93	0.007
TS	2	3.383	1.691	26.55	0.036
Error	2	0.127	0.064		
Total	8	676.101			

Table 6: ANOVA table for specimen with ZnO as reinforcement

Source	DF	Adj SS	Adj MS	F-Value	P-Value
PWJ	2	756.471	378.236	179.06	0.006
SoD	2	37.864	18.932	8.96	0.100
TS	2	12.906	6.453	3.05	0.247

Error	2	4.225	2.112		
Total	8	811.466			

Table 7: ANOVA table for specimen with B_4C as reinforcement

Source	**DF**	**Adj SS**	**Adj MS**	**F-Value**	**P-Value**
PWJ	2	742.937	371.469	314.57	0.003
SoD	2	26.905	13.453	11.39	0.081
TS	2	0.216	0.108	0.09	0.916
Error	2	2.362	1.181		
Total	8	772.420			

Table 8: ANOVA table for specimen with MgO as reinforcement

Source	**DF**	**Adj SS**	**Adj MS**	**F-Value**	**P-Value**
PWJ	2	750.036	375.018	195.95	0.005
SoD	2	25.914	12.957	6.77	0.129
TS	2	9.477	4.739	2.48	0.288
Error	2	3.828	1.914		
Total	8	789.255			

Table 9: ANOVA table for specimen with B_4N as reinforcement

Source	**DF**	**Adj SS**	**Adj MS**	**F-Value**	**P-Value**
PWJ	2	753.490	376.745	850.46	0.001
SoD	2	41.568	20.784	46.92	0.021
TS	2	9.864	4.932	11.13	0.082
Error	2	0.886	0.443		
Total	8	805.807			

Following points are observed from the ANOVA tables

i. PWJ is a significant factor for removing material for Al7075 composite which is reinforced with TiO_2, ZnO, B_4C, MgO, and B_4N by AWJM.

ii. SoD is a significant factor for removing material for Al7075 composite which is reinforced with TiO_2, and B_4N by AWJM.

iii. On the other hand, TS is a significant factor for removing material for Al7075 composite which is reinforced with B_4N by AWJM.

iv. The computed F-value for SoD and TS in computing MRR is smaller than the tabulated F-value. Itimplies that the change in measure of MRR valuedue to change in the level of one process parameter isindependent of the other process parameters.

5.2. Result from Taguchi S/N analysis

The effect of 3 factors viz. PWJ, SoD and TS are studied in this paper. The S/N ratio values for the experiments conducted for the 5 specimen is tabulated in table 10. Figure 7 – 11 shows the main effect plots for the means and S/N ratio values for the 5 specimen prepared for the study. The conclusion drawn from the figures are summarized as follows:

Table 10: S/N values

Exp. no.	**S/N values**				
	AL7075+TiO_2	**AL7075+ZnO**	**AL7075+B_4C**	**AL7075+MgO**	**AL7075+B_4N**
1	14.89368127	11.37107424	5.348128	5.348128	11.37107
2	15.5107527	15.5107527	11.98893	11.98893	15.51075
3	17.45710489	17.45710489	14.95911	14.95911	17.4571
4	21.93820026	21.93820026	21.9382	20	21.9382
5	23.0567702	23.0567702	23.05677	23.05677	24.39536
6	24.86076097	26.02059991	24.86076	24.86076	26.0206
7	27.95880017	27.95880017	27.9588	27.9588	27.9588
8	28.84708646	29.76226764	27.824	28.84709	29.76227
9	29.11850882	29.11850882	29.11851	28.20339	29.11851

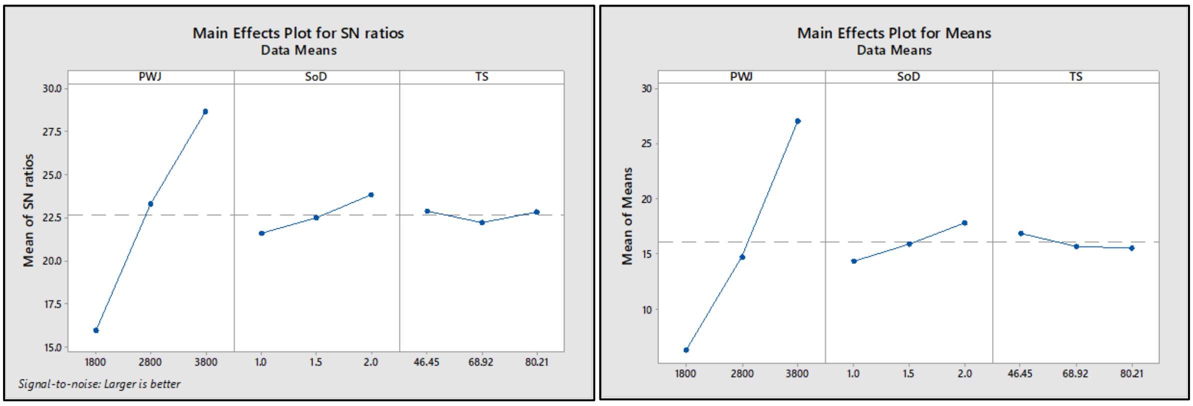

(a) (b)

Figure 7: Main effectplot for (a) S/N ratio and (b) meansfor specimen with TiO_2as reinforcement

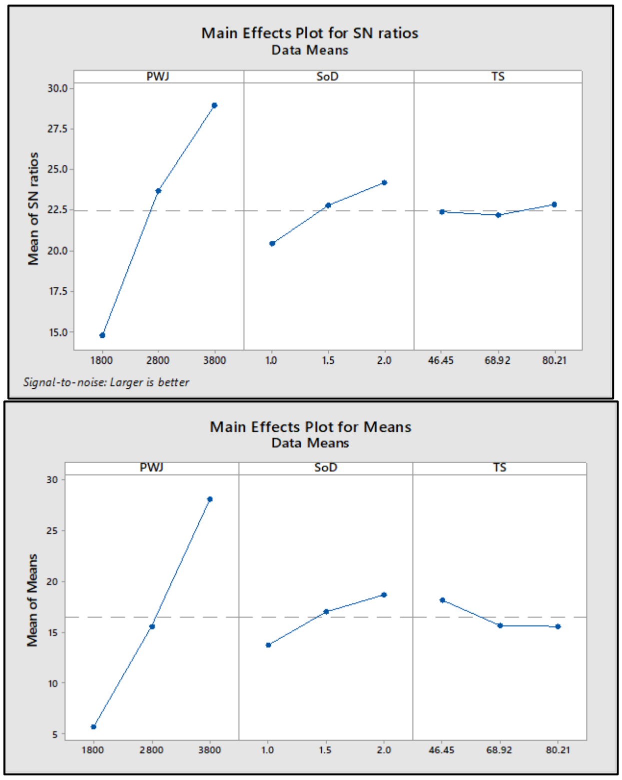

(a) (b)

Figure 8: Main effectplot for (a) S/N ratio and (b) meansfor specimen with ZnOas reinforcement

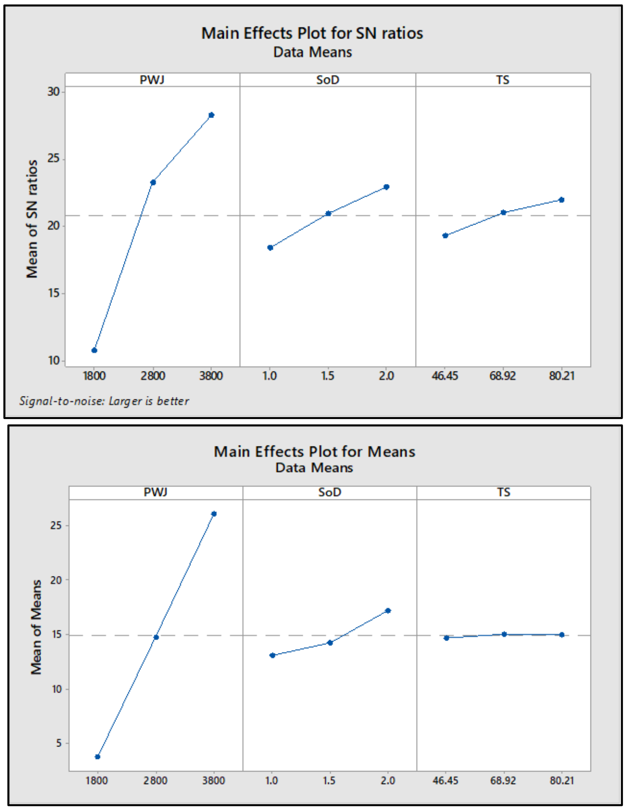

(a) (b)

(b) Figure 9: Main effectplot for (a) S/N ratio and (b) meansfor specimen with B_4Cas reinforcement

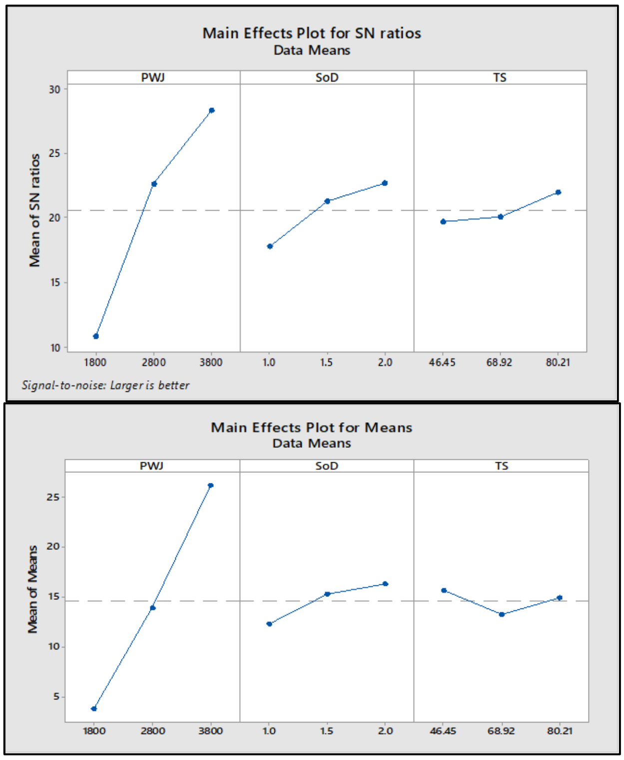

(a) (b)

Figure 10: Main effectplot for (a) S/N ratio and (b) meansfor specimen with MgOas reinforcement

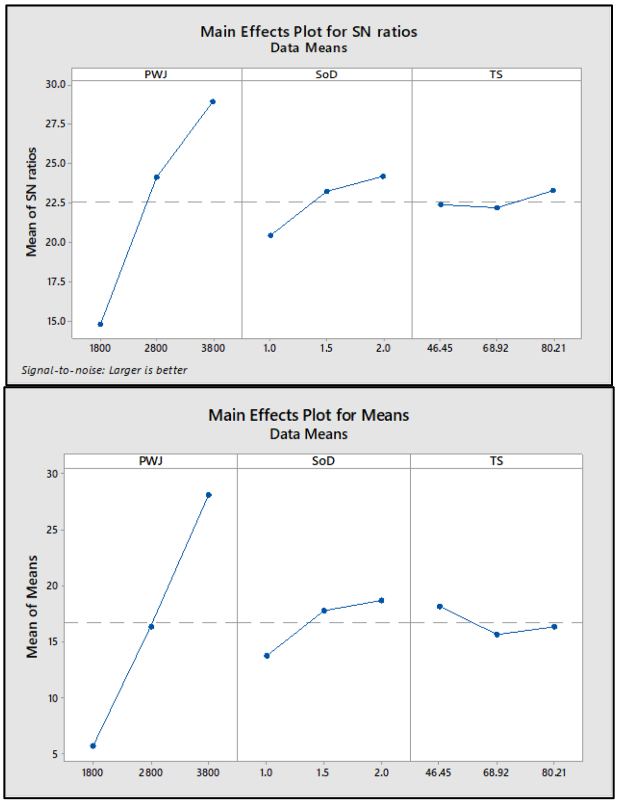

(a) (b)

Figure 11: Main effectplot for (a) S/N ratio and (b) meansfor specimen with B_4N as reinforcement

Table 11:Optimum level combination of parameters for maximum MRR for different reinforcements

	PWJ (bar)	SoD (mm)	TS (mm/min)
AL7075+TiO_2	3800	2	68.92
AL7075+ZnO	3800	1.5	46.45
AL7075+B_4C	3800	2	68.92
AL7075+MgO	3800	1.5	46.45
AL7075+B_4N	3800	1.5	46.45

5.2.1. Effect of PWJ on MRR

From figure 7 – 11, it is observed that higher value of PWJ is preferred for removing material per minute from the work-piece. Pressure plays a significantly impacts cutting performance. Increased pressure results in a faster, more efficient process by raising the jet's velocity and MRR.In AWJM, pressure influences the efficient suspension and delivery of abrasive particles.

5.2.2. Effect of SoD on MRR

From figure 7 – 11, it is observed that high value of SoD is preferred for removing material per minute from the work-piece. It is due to the fact that the increase in SoD value increases the width of cut up and also the width nozzle distance and these two factors are important for material removing from the specimen.

5.2.3. Effect of TS on MRR

From figure 7 – 11, it is observed that the TS does not make a significant impact for removing material per minute from the work-piece as compared to PWJ and SoD. This is due to the fact that at high speed less abrasives hit the specimen which in turn removes less material from it. Since less abrasives hit the specimen the smooth cutting depth also decreases significantly thereby decreasing the MRR value [18].

5.3. Result of the Contour plot analysis

The contour plot is a 2D view of the 3D graphical representation plotted for constant z-slices. The governing equations for producing the contour plot is achieved from the regression equations generated by the RSM. The regression equations generated by RSM is a second-degree polynomial. The regression equations developed for this study is given in Eqs. (5 – 9).

$$MRR_{TiO_2} = 4.113 - 0.001492\,\mathrm{PWJ} + 5.106\,\mathrm{SoD} - 0.2254\,\mathrm{TS} + 0.000002\,\mathrm{PWJ}^2 - 0.2480\,\mathrm{SoD}^2 + 0.001040\,\mathrm{TS}^2 - 0.000214\,\mathrm{PWJ} * \mathrm{SoD} + 0.000018\,\mathrm{PWJ} * \mathrm{TS} \quad (5)$$

$$MRR_{ZnO} = -27.43 + 0.007897\,\mathrm{PWJ} + 23.51\,\mathrm{SoD} - 0.008966\,\mathrm{TS} + 0.000001\,\mathrm{PWJ}^2 - 3.343\,\mathrm{SoD}^2 - 0.001004\,\mathrm{TS}^2 - 0.003020\,\mathrm{PWJ} * \mathrm{SoD} + 0.000005\,\mathrm{PWJ} * \mathrm{TS} \quad (6)$$

$$MRR_{B_4C} = -26.33 + 0.007354\,\mathrm{PWJ} + 10.99\,\mathrm{SoD} + 0.1398\,\mathrm{TS} + 0.000000\,\mathrm{PWJ}^2 - 0.1541\,\mathrm{SoD}^2 - 0.003100\,\mathrm{TS}^2 - 0.001847\,\mathrm{PWJ} * \mathrm{SoD} + 0.000084\,\mathrm{PWJ} * \mathrm{TS} \quad (7)$$

$$MRR_{MgO} = -18.04 + 0.006068\,\mathrm{PWJ} + 37.04\,\mathrm{SoD} - 0.6437\,\mathrm{TS} + 0.000001\,\mathrm{PWJ}^2 - 7.253\,\mathrm{SoD}^2 + 0.002917\,\mathrm{TS}^2 - 0.003656\,\mathrm{PWJ} * \mathrm{SoD} + 0.000071\,\mathrm{PWJ} * \mathrm{TS} \quad (8)$$

$$MRR_{B_4N} = -20.04 + 0.009950\ \mathrm{PWJ} + 28.56\ \mathrm{SoD} - 0.4870\ \mathrm{TS} + 0.000001\ \mathrm{PWJ}^2 - 6.502\ \mathrm{SoD}^2 + 0.003140\ \mathrm{TS}^2 - 0.001441\ \mathrm{PWJ} * \mathrm{SoD} + 0.000005\ \mathrm{PWJ} * \mathrm{TS} \quad (9)$$

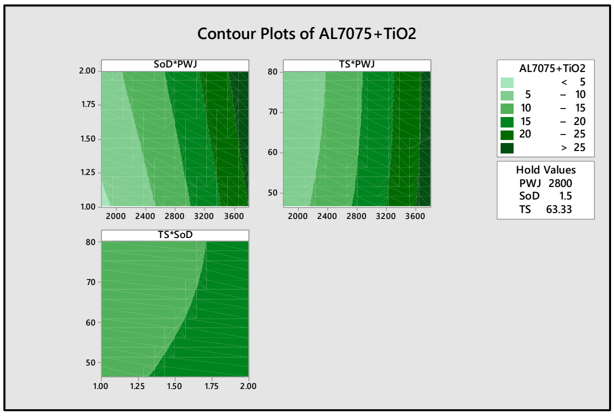

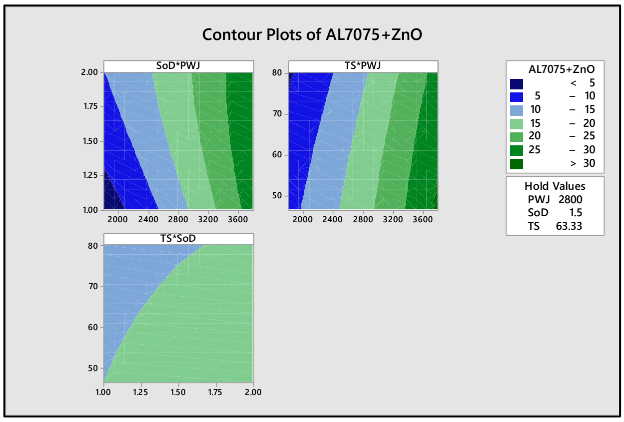

Figure 12: Contour plot for specimen with TiO_2 Figure 13: Contour plot for specimen with ZnO

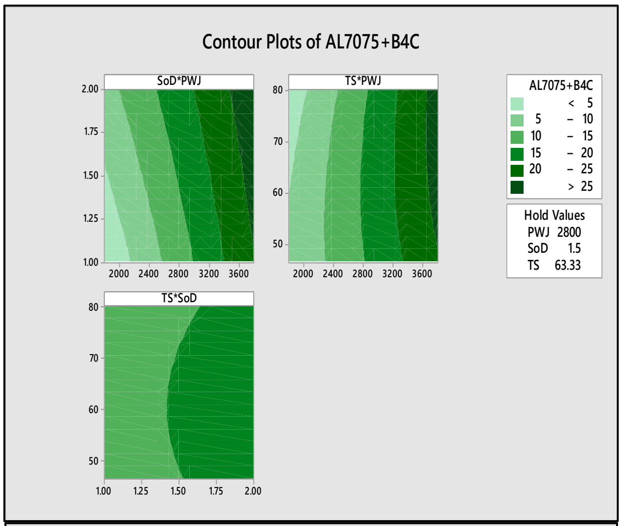

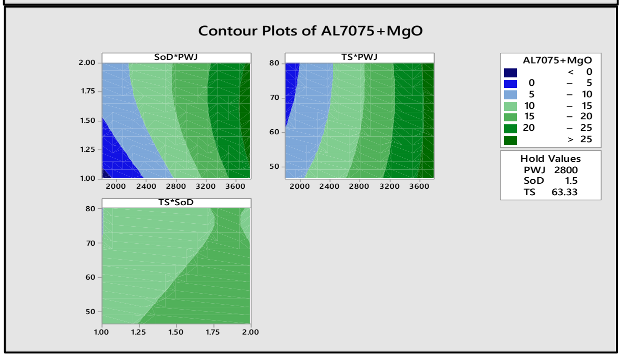

Figure 14: Contour plot for specimen with B_4CFigure 15: Contour plot for specimen with MgO

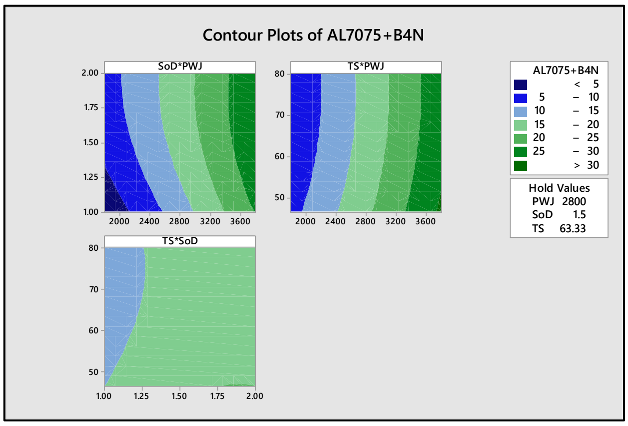

Figure 16: Contour plot for specimen with B_4N

Following points are observed from figure 12 – 16:

i. MRR is more for the specimen reinforced with TiO_2, ZnO, B_4C and B_4N when the PWJ value is high but
   a. Same MRR value can be attained by decreasing the PWJ and increasing the SoD value.
   b. Same MRR value can be attained at lower PWJ and TS value.

ii. MRR is more for the specimen reinforced with MgO when the PWJ value is high but there is an optimal range for SoD.

iii. MRR value is more for high PWJ value and least TS value the specimen reinforced withZnO, and B_4N.

iv. MRR is more for the specimen reinforced with B_4C when the PWJ value is high but there is an optimal range for TS.

5.4. Result from trade-off analysis

Tuijin Jishu/Journal of Propulsion Technology
ISSN: 1001-4055
Vol. 45 No. 3 (2024)

The composite desirability value is computed by the MORSM value to get the optimal machining parameter settings that would maximize the MRR value for all the specimens with reinforcement as TiO_2, ZnO, B_4C, MgO and B_4N. Figure 17 shows MORSM model developed by Minitab 17 software.

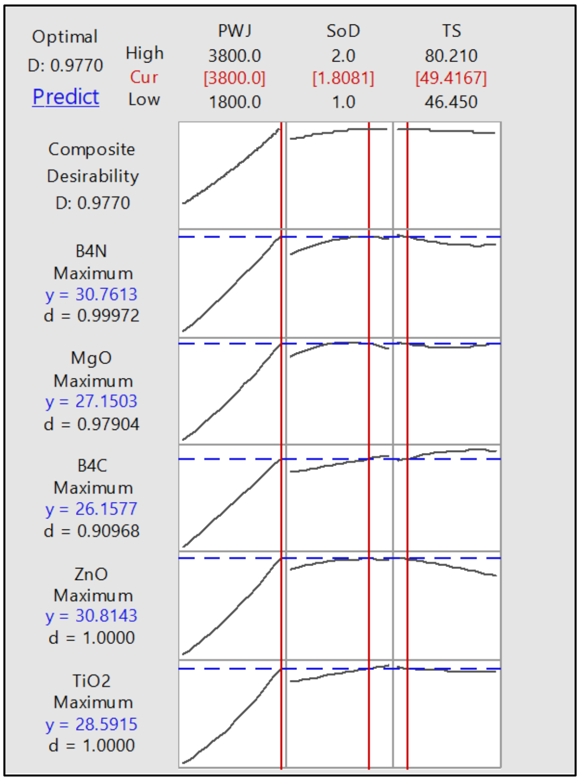

Figure 17:MORSM model developed by Minitab 17 software

The value of composite desirability computed for the model is 0.9770 for PWJ $= 3800\ bar$, SoD $= 1.8081 mm$ and TS $= 49.4167\ mm/min$.

5.5. Validation of the optimal result

5.5.1. Experimental validation of the optimal result

For validation the result obtained from the MORSM model an experiment is conducted in parameters nearer to the optimal values obtained from the model. The reason for conducting the experiment at the nearer value is availability of the particular value in the experimental equipment. The values at which validation experiment is conducted are PWJ $= 3800\ bar$, SoD $= 1.8\ mm$ and TS $= 49.42\ mm/min$. The output obtained from the MORSM model and experimentation are compared by computing the mean absolute percentage error (MAPE) as per Eq. (10).

$$e = \frac{|y - y_m|}{y_m} \times 100\% \qquad (10)$$

Where y and y_m is the MRR value obtained from experimentation and model respectively. On the other hand, e is the MAPE value. The comparison table for the validation experiment is shown in table 12.

Table 12: Comparison table for the validation experiment

Sl. no.	y	y_m	e (%)
1	29.78	30.7638	3.198

2	29.00	27.1744	6.718
3	27.80	26.1305	6.389
4	32.00	30.8143	3.848
5	26.72	28.5639	6.455

From table 12, it is observed that the MAPE value computed from the model and the experiment is 3.198%, 6.718%, 6.389%, 3.848% and 6.455% for the specimen reinforced with TiO_2, ZnO, B_4C, MgO and B_4N respectively.

6. Conclusions

Optimizing factors in AWJM is pivotal for enhancing precision and efficiency in material processing. Tailoring abrasive material selection, nozzle design, pressure, feed rate, and path planning to specific requirements ensures superior results. Real-time monitoring and environmental considerations are also vital. Safety measures must be upheld. By systematically fine-tuning these factors, AWJM enables precise, cost-effective, and environmentally friendly material cutting, making it an indispensable tool in modern manufacturing.

In this study, the effect of PWJ, SoD and TS on the MRR is studied as it directly correlates with the efficiency of the machining. Higher MRR indicates that more material is removed in a shorter time, which is usually desirable in industrial applications to meet production targets and reduce manufacturing costs.

The finding drawn from the analysis are summarized as follows:

i. PWJ is a significant factor for removing material. Whereas, SoD plays a significant role for removing material for Al7075 composite which is reinforced with TiO_2, and B_4N. However, TS is the least important factor for removing material from Al7075 composite by AWJM. This is because at high speed less abrasives hit the specimen which results in less cutting depth and as a result less material is removed from the workpiece.

ii. MRR is more for the specimen reinforced with TiO_2, ZnO, B_4C and B_4N when the PWJ value is high. However, the same MRR value can be obtained by simultaneously decreasing the PWJ and increasing the SoD value. Also the same MRR value can be obtained by simultaneously lowering PWJ and TS value.

iii. From table 4 and 11, it is evident that the MRR for specimen reinforced with ZnO and B_4N is the highest when PWJ $= 3800\, bar$, SoD $= 1.5 mm$ and TS $= 46.45\, mm/min$. Whereas MRR is highest for specimen reinforced with TiO_2, MgO and B_4C is the highest when PWJ $= 3800\, bar$, SoD $= 2\, mm$ and TS $= 68.92\, mm/min$. It can be noted that the PWJ value for MRR is common for all the prepared specimens. However, the SoD and TS value is different. Therefore, in order to compute a common machining parameters for all the specimens, the problem is set in a multi-objective optimization environment.

iv. From table 4 and table 12, it can be noted that better MRR values are obtained for certain machining parameters. However, it should be noted that the MRR for other specimens for that machining parameter is not optimal. Due to this reason, a common machining parameters is to be determined that provide a near optimal MRR value for all the 5 different MMC specimen prepared.

v. The common optimized values for the process parameters are PWJ $= 3800\, bar$, SoD $= 1.8\, mm$ and TS $= 49.42\, mm/min$. The MRR value computed from this is a trade-off value in between the best and the second best experimental values. The difference in the best MRR value and trade-off MRR value is very less and it will not impact the machining productivity.

vi. An experimental validation is carried out to check the feasibility of the result obtained from MORSM model. The error computed between the simulated and experimental result varied in between 3.198% to 6.718% which is within the controllable limit. Hence, it can be concluded that the method developed is suitable to determine the optimized value of process parameters by AWJM.

References:

1. Thompson, M., Ferguson, B., Nielson, G. N., & Schultz, S. (2022, May). Machining of Silicon Carbide Wafers. In *2022 Intermountain Engineering, Technology and Computing (IETC)* (pp. 1-5). IEEE.

2. Natarajan, Y., Murugesan, P. K., Mohan, M., & Khan, S. A. L. A. (2020). Abrasive Water Jet Machining process: A state of art of review. *Journal of Manufacturing Processes*, *49*, 271-322.
3. Tercan, H., &Meisen, T. (2022). Machine learning and deep learning based predictive quality in manufacturing: a systematic review. *Journal of Intelligent Manufacturing*, *33*(7), 1879-1905.
4. Hussain, S. A. I., Sen, B., Das Gupta, A., &Mandal, U. K. (2020). Novel multi-objective decision-making and trade-off approach for selecting optimal machining parameters of inconel-800 superalloy. *Arabian Journal for Science and Engineering*, *45*, 5833-5847.
5. Singh, R., Hussain, S. A. I., Dash, A., &Rai, R. N. (2020). Modelling and optimizing performance parameters in the wire-electro discharge machining of Al5083/B 4 C composite by multi-objective response surface methodology. *Journal of the Brazilian Society of Mechanical Sciences and Engineering*, *42*, 1-32.
6. Moayyedian, M., Mohajer, A., Kazemian, M. G., Mamedov, A., &Derakhshandeh, J. F. (2020). Surface roughness analysis in milling machining using design of experiment. *SN Applied Sciences*, *2*, 1-9.
7. Bhirud, N. L., Dube, A. S., Patil, A. S., &Bhole, K. S. (2023). Multi-objective optimization of cutting parameters and helix angle for temperature rise and surface roughness using response surface methodology and desirability approach for Al 7075. *International Journal on Interactive Design and Manufacturing (IJIDeM)*, 1-20.
8. Dutta, S., &Narala, S. K. R. (2021). Optimizing turning parameters in the machining of AM alloy using Taguchi methodology. *Measurement*, *169*, 108340.
9. Öztürk, B., & Kara, F. (2020). Calculation and estimation of surface roughness and energy consumption in milling of 6061 alloy. *Advances in Materials Science and Engineering*, *2020*, 1-12.
10. Emembolu, L. N., Ohale, P. E., Onu, C. E., &Ohale, N. J. (2022). Comparison of RSM and ANFIS modeling techniques in corrosion inhibition studies of Aspilia Africana leaf extract on mild steel and aluminium metal in acidic medium. *Applied Surface Science Advances*, *11*, 100316.
11. Kaushik, A., Arif, M., Tumula, P., &Ebohon, O. J. (2020). Effect of thermal comfort on occupant productivity in office buildings: Response surface analysis. *Building and Environment*, *180*, 107021.
12. Fu, J., Zang, C., & Zhang, J. (2020). Economic and resource and environmental carrying capacity trade-off analysis in the Haihe River basin in China. *Journal of Cleaner Production*, *270*, 122271.
13. Comont, D., Lowe, C., Hull, R., Crook, L., Hicks, H. L., Onkokesung, N., ...&Neve, P. (2020). Evolution of generalist resistance to herbicide mixtures reveals a trade-off in resistance management. *Nature communications*, *11*(1), 3086.
14. Banihashemi, S. A., Khalilzadeh, M., Shahraki, A., Malkhalifeh, M. R., &Ahmadizadeh, S. S. R. (2021). Optimization of environmental impacts of construction projects: a time–cost–quality trade-off approach. *International Journal of Environmental Science and Technology*, *18*, 631-646.
15. Liu, C., & Yang, H. (2022). Multi-objective optimization of a concrete thermal energy storage system based on response surface methodology. *Applied Thermal Engineering*, *202*, 117847.
16. Senthil, S. M., Parameshwaran, R., Ragu Nathan, S., Bhuvanesh Kumar, M., &Deepandurai, K. (2020). A multi-objective optimization of the friction stir welding process using RSM-based-desirability function approach for joining aluminum alloy 6063-T6 pipes. *Structural and Multidisciplinary Optimization*, *62*, 1117-1133.
17. Delacre, M., Leys, C., Mora, Y. L., &Lakens, D. (2019). Taking parametric assumptions seriously: Arguments for the use of Welch's F-test instead of the classical F-test in one-way ANOVA. *International Review of Social Psychology*, *32*(1), 13.
18. Hascalik, A., Çaydaş, U., &Gürün, H. (2007). Effect of traverse speed on abrasive waterjet machining of Ti–6Al–4V alloy. *Materials & Design*, *28*(6), 1953-1957.
19. Syazwani, H., Mebrahitom, G., &Azmir, A. (2016, February). A review on nozzle wear in abrasive water jet machining application. In *IOP Conference Series: Materials Science and Engineering* (Vol. 114, No. 1, p. 012020). IOP Publishing.
20. Perec, A. (2021). Research into the disintegration of abrasive materials in the abrasive water jet machining process. *Materials*, *14*(14), 3940.

21. Mohamad, W. N. F., Kasim, M. S., Norazlina, M. Y., Hafiz, M. S. A., Izamshah, R., & Mohamed, S. B. (2020). Effect of standoff distance on the kerf characteristic during abrasive water jet machining. *Results in Engineering*, *6*, 100101.
22. Natarajan, Y., Murugesan, P. K., Mohan, M., & Khan, S. A. L. A. (2020). Abrasive Water Jet Machining process: A state of art of review. *Journal of Manufacturing Processes*, *49*, 271-322.
23. Abushanab, W. S., Moustafa, E. B., Harish, M., Shanmugan, S., &Elsheikh, A. H. (2022). Experimental investigation on surface characteristics of Ti6Al4V alloy during abrasive water jet machining process. *Alexandria Engineering Journal*, *61*(10), 7529-7539.
24. Llanto, J. M., Tolouei-Rad, M., Vafadar, A., &Aamir, M. (2021). Recent progress trend on abrasive waterjet cutting of metallic materials: a review. *Applied Sciences*, *11*(8), 3344.
25. Joel, C., &Jeyapoovan, T. (2021). Optimization of machinability parameters in abrasive water jet machining of AA7075 using Grey-Taguchi method. *Materials Today: Proceedings*, *37*, 737-741.
26. Kumar, G. K., Arunachalam, M., Abinash, B., & Kumar, B. K. (2018). Optimization of Abrasive Water Jet Machining Process Parameters for Duplex Stainless Steel-2205 by Using Response Surface Methodology. *International Journal of Scientific Research in Mechanical and Materials Engineering*, *2*(3), 17-28.
27. Rao, R. V., Rai, D. P., &Balic, J. (2019). Multi-objective optimization of abrasive waterjet machining process using Jaya algorithm and PROMETHEE Method. *Journal of Intelligent Manufacturing*, *30*, 2101-2127.
28. Marichamy, S., Ravichandran, M., Stalin, B., &Babu, S. B. (2019). Optimization of abrasive water jet machining parameters for α-β brass using Taguchi methodology. *FME Transactions*, *47*(1), 116-121.
29. Murugabalaji, V., Kanthababu, M., Jegaraj, J., &Saikumar, S. (2014). Multi-objective optimization of abrasive waterjet machining process parameters using particle swarm technique. *International Journal of Materials Forming and Machining Processes (IJMFMP)*, *1*(2), 62-79.
30. Shukla, R., & Singh, D. (2017). Experimentation investigation of abrasive water jet machining parameters using Taguchi and Evolutionary optimization techniques. *Swarm and Evolutionary Computation*, *32*, 167-183.
31. Ahmed, A. A. M., &Qian, J. (2020). A Review on Abrasive Water Jet Cutting Machining Due to Optimization, Advantages, Weakness and Future Directions. *Ijsret. Com*, *6*(3), 1127-1136.
32. Deresse, N. C., Deshpande, V., & Taifa, I. W. (2020). Experimental investigation of the effects of process parameters on material removal rate using Taguchi method in external cylindrical grinding operation. *Engineering Science and Technology, an International Journal*, *23*(2), 405-420.
33. Ozcan, Y., Tunc, L. T., Kopacka, J., Cetin, B., & Sulitka, M. (2021). Modelling and simulation of controlled depth abrasive water jet machining (AWJM) for roughing passes of free-form surfaces. *The International Journal of Advanced Manufacturing Technology*, *114*(11), 3581-3596.
34. Yue, Z., Huang, C., Zhu, H., Wang, J., Yao, P., & Liu, Z. (2014). Optimization of machining parameters in the abrasive waterjet turning of alumina ceramic based on the response surface methodology. *The International Journal of Advanced Manufacturing Technology*, *71*, 2107-2114.
35. Altin Karataş, M., Gökkaya, H., Akincioğlu, S., & Biberci, M. A. (2022). Investigation of the effect of AWJ drilling parameters for delamination factor and surface roughness on GFRP composite material. *Multidiscipline Modeling in Materials and Structures*, *18*(4), 734-753.